NANO LETTERS

Letter

pubs.acs.org/NanoLett

Enhanced Photoelectrochemical Hydrogen Production from Silicon Nanowire Array Photocathode

Ilwhan Oh,*[,†,§] Joohong Kye,[‡,§] and Seongpil Hwang*[,‡,§]

[†]K.A.N.C., Suwon, Gyeonggi 443-270, Republic of Korea

[‡]Department of Chemistry, Myongji University, Yongin 449-728, Republic of Korea

Supporting Information

ABSTRACT: Herein we report that silicon nanowires (SiNWs) fabricated via metal-catalyzed electroless etching yielded a photoelectrochemical hydrogen generation performance superior to that of a planar Si, which is attributed to a lower kinetic overpotential due to a higher surface roughness, favorable shift in the flat-band potential, and light-trapping effects of the SiNW surface. The SiNW photocathode yielded a photovoltage of 0.42 V, one of the highest values ever reported for hydrogen generation on p-type Si/electrolyte interfaces.

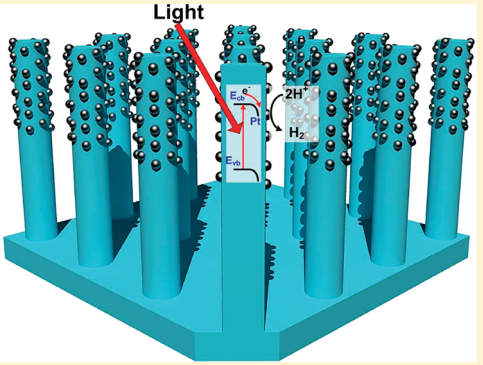

KEYWORDS: *Silicon nanowire, metal-catalyzed electroless etching, photoelectrochemistry, hydrogen evolution reaction, solar water splitting*

Hydrogen fuel may be produced directly from water and sunlight in a process that can potentially be used as a method for storing energy for emission-free, sustainable future energy generation.[1−4] In photoelectrochemical water splitting, the cathode and/or anode of an electrochemical cell is composed of a light-absorbing material, such as a semiconductor. A photoelectrochemical cell uses photon energy to generate H_2 at a cathode and O_2 at an anode, as described in the following half-cell reactions

$$2H^+ + 2e^- \rightarrow H_2 \text{ (cathode)} \quad (1a)$$

$$H_2O \rightarrow \frac{1}{2}O_2 + 2H^+ + 2e^- \text{ (anode)} \quad (1b)$$

The Gibbs free energy change ΔG° of the net reaction is 237 kJ/mol, or equivalently, the standard emf, ΔE° is −1.23 V. As the negative emf indicates, the net reaction is energetically uphill reaction. Thus, to achieve unassisted (no external bias) water splitting, a minimum photovoltage of 1.23 V must be supplied by a photoelectrode to drive the water splitting reaction. From a photoelectrochemistry perspective, the important aspects of solar water splitting cells are (i) the thermodynamics at semiconductor/liquid interface, such as the band gap, band bending, and band edge energy for light absorption and charge transport; (ii) the kinetics of charge transfer at the semiconductor/electrolyte interface; (iii) carrier recombination at the interface; (iv) the reflection of light at the interfaces; and (v) the costs and stability of the semiconductor electrode.

Silicon is a widely abundant relatively low-cost semiconductor material most widely used in photovoltaic devices, which are associated with a vast knowledge base and manufacturing infrastructure.[5] Photoelectrochemical H_2 generation at Si/electrolyte interfaces has been studied for decades.[6−10] Slow electrode kinetics during the hydrogen evolution reaction (HER) on Si surfaces has led research efforts to modify surfaces with electrocatalysts, such as Pt, to facilitate HER. A fundamental problem with using low-band gap Si as a photocathode for H_2 generation is that the difference between the Si valence band edge and the H^+/H_2 redox level is small, which limits the photovoltage. To address this problem, n^+/p-Si junctions have been introduced to increase the photovoltage by enhancing band bending.[9,10] Tandem water splitting cells are envisioned in which a small band gap semiconductor, such as p-type Si, and a high band semiconductor are connected in series, thereby overcoming the water-splitting voltage threshold of 1.23 V and more efficiently utilizing the solar spectrum.[4]

Although most previous studies have focused on planar semiconductor/electrolyte interfaces, recent advances in nanofabrication have enabled the adoption of nanostructured semiconductors in photoelectrochemical devices.[1,4] Among the various nanostructures, nanowire geometry is especially interesting and intriguing. Vertically aligned nanowires should be able to decouple minority carrier generation and

Received: October 10, 2011
Revised: November 17, 2011
Published: December 5, 2011

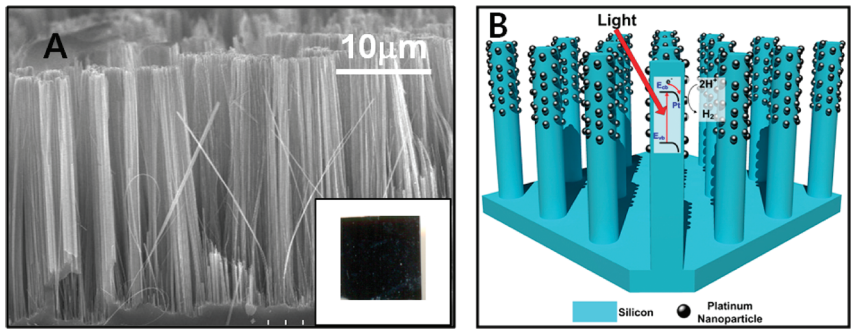

Figure 1. (A) Si nanowire array fabricated by metal-catalyzed chemical etching imaged with scanning electron microscope. Inset: photograph of ~10 mm × 10 mm sample of SiNW with low reflection. (B) Schematic of Si nanowire array photoelectrode. Photon absorbed by Si nanowire generates minority carrier (electron), which drifts to semiconductor/electrolyte interface where H_3O^+ is reduced to H_2. Si nanowire is impregnated with Pt nanoparticles that serve as electrocatalysts for the electrode reaction.

collection.[4,10−12] That is, when a nanowire array is vertically aligned, incident photons are absorbed, and minority carriers are generated along the length of the nanowires. Minority carriers then need only to travel a short distance along the nanowire diameter before being collected at the junction, a merit that would allow the use of low-cost, low-quality semiconductor materials. However, solar energy conversion devices that utilize nanowires have thus far exhibited modest to low performances, presumably due to a dramatically higher rate of surface recombination and the presence of shunt paths.[13−22] A recent study of chemically grown Si nanowires indicates that, depending on the growth conditions, impurities and defects in nanowires can generate surface trap states that lower the performance of devices based on nanowires.[23] Reduced open-circuit voltages due to the higher interface area may provide another reason for the low performance as well.[4]

Here, we report the photoelectrochemical generation of H_2 using a p-type Si nanowire (SiNW) array photocathode, which was fabricated via metal-catalyzed electroless etching (MCEE) followed by impregnation with a Pt nanoparticle (NP) electrocatalyst. We were motivated to investigate the Pt/Si NW array photocathodes for several reasons. First, the nanostructured photoelectrodes should display dramatically higher semiconductor/electrolyte interface areas, which can reduce the overpotential due to the slow H_2 generation kinetics at the electrode. Second, because the dimensions of the SiNW array are comparable to the wavelength of visible light, the SiNW array should function as an antireflective or light-trapping layer to minimize reflection of incident photons, thereby enhancing the photocurrent and/or photovoltage.[19] In addition, nanostructuring can introduce changes in the semiconductor energetics that can enhance the semiconductor/electrolyte characteristics. As described below, the Pt/SiNW photocathode showed a surprising increase in the photovoltage relative to conventional Pt/planar Si photocathodes. Electrochemical characterization of the Pt/Si NW photoelectrodes was conducted to investigate the mechanism underlying the enhanced performance. Although some reports have described the use of porous Si for H_2 generation,[24,25] to our knowledge this is the first report to investigate H_2 generation on Pt/SiNW photocathodes.

Among the various methods for fabricating semiconductor nanowires, the vapor−liquid−solid (VLS) method is widely used as a bottom-up approach.[26,27] An alternative top-down approach, MCEE,[28−30] provides a unique and simple method for fabricating Si nanowire. In the MCEE method, a thin metal (usually Ag) seed layer is first deposited onto a Si surface, and the seed-covered Si material is submitted to electroless etching in a mixture of H_2O_2 and HF (see the Supporting Information for details). Figure 1 shows the structure of a SiNW array fabricated by electroless etching of p-type Si(100) (B-doped; resistivity = 10 Ω·cm) for 30 min. Figure 1A shows an SEM image of a dense array of SiNWs vertically aligned on the original substrate, similar to the results reported previously.[28−30] The average diameter of the SiNWs was 100 nm, and the average length was 20 μm after 30 min of etching. After selective removal of the residual Ag seed layer in HNO_3, the SiNW is impregnated with Pt NPs by immersion of the SiNW into a solution containing 0.4 M HF and 1 mM K_2PtCl_6. The Pt NPs function as an electrocatalyst for H_2 generation. The optimum deposition time was found to be 9 min. Previous studies found that electroless deposition produced Pt NPs of diameter 5−10 nm located mainly near the ends of the SiNW tips.[31] Figure 1B shows a schematic diagram of H_2 generation on the Pt/SiNW array photocathode immersed in an acid solution and irradiated with sunlight. The SiNWs absorb incident photons and generate minority carriers (electron) that flow across the SiNW/electrolyte interface and reduce H^+ into H_2.

Figure 2 shows current density (J)−electrode potential (E) measurements for H_2 generation on a p-type SiNW photocathode in a stirred solution containing H_2SO_4 and 0.5 M K_2SO_4 (pH 1). A three-electrode configuration is used with an epoxy-sealed SiNW photocathode, a Pt counter electrode, and a standard calomel reference electrode (SCE) (see Supporting Information for details). A calibrated halogen lamp illuminates the SiNW photocathode surface with 100-mW/cm^2 simulated solar radiance. For reference, identical photoelectrochemical measurements were performed using a planar p-type Si photocathode. Figure 2A shows that the bare planar Si exhibited a very small photocurrent for H_2 generation until E reached −0.5 V because without an electrocatalyst present on the Si surface, electron transfer from the Si surface to H^+ was very slow. In contrast, the SiNW photocathode generated a much higher photocurrent (solid line in Figure 2A). The fact that the photocurrent generated on the SiNW substrate under dark conditions (dashed line) was almost zero confirmed that the current observed upon illumination of the SiNW was photogenerated. Most notably, the onset potential (E_{OS}) on the SiNWs was 0.2 V, more positive than that on the planar Si.

Figure 2B shows the J−E measurements for a Pt NP-impregnated Si photoelectrode. In the presence of Pt NPs on

dx.doi.org/10.1021/nl203564s | Nano Lett. 2012, 12, 298−302

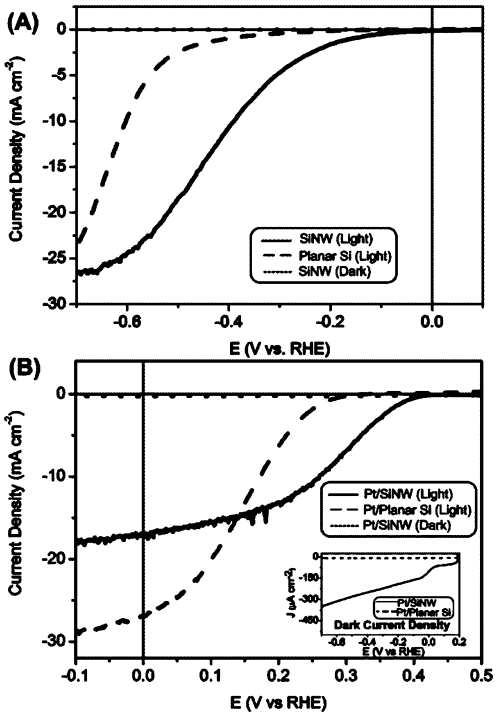

Figure 2. Photoelectrochemical H_2 generation on p-type Si NW array electrode (both illuminated and dark) in a stirred solution of H_2SO_4 + 0.5 M K_2SO_4 (pH 1). Same measurements on planar p-type Si are performed for reference. (A) Bare SiNW and planar Si photocathodes. While planar Si gives little photocurrent in positive photovoltage region, SiNW shows dramatic boost in photocurrent of H_2 generation. (B) When SiNW is impregnated with Pt nanoparticle by electroless deposition, overpotential for H_2 generation is significantly reduced both for SiNW and planar Si. Photovoltage of SiNW is ~0.2 V larger than that of planar Si. The inset shows the dark current densities of Pt NP-impregnated SiNW and planar Si electrode in the same electrolyte.

the Si surface, H_2 generation from the photoelectrodes was greatly enhanced due to the facile reduction of H^+ at the Pt electrocatalyst. The E_{OS} value for the Pt/SiNW was positively shifted to 0.42 V, which was much larger than the photovoltage of 0.33 V for the Pt/planar Si. To our knowledge, this photovoltage for the Pt/SiNW is the highest value ever reported for the generation of H_2 at a p-type Si/electrolyte interface. Because a photovoltage of at least 1.23 V is required to drive unassisted water splitting, this enhanced photovoltage on the SiNW photocathode will relieve the burden on the photoanode in a tandem-cell configuration, in which water oxidation usually exhibits a large kinetic overpotential. Furthermore, the Pt/SiNW photoelectrode showed a robust temporal stability of photocurrent in a longer time scale, which would be critical in practical application (see Figure S2 in Supporting Information). The inset of Figure 2B shows that the dark current density for the Pt/SiNW was much larger than that for the Pt/planar Si photocathode, which was due to a larger surface area of the Pt/SiNW. In purely solid-state solar cells, a larger dark current normally leads to lower photovoltage.[5] On the contrary, in current work and other report involving nanostructured semiconductor/electrolyte interfaces,[25] an E_{OS} enhancement was observed despite the higher dark current. For the SiNW/electrolyte interface where hydrogen evolution reaction occurs, it seems that additional factors have a significant effect on the E_{OS} value. As we tried to verify in the following measurements, those factors include kinetic overpotential and double layer potential, which are not taken into consideration in the pure solid-state junction theory. The net increment of E_{OS} in the SiNW/electrolyte interface indicates that the photovoltage reduction by the higher dark current was overcome by an E_{OS} enhancement by these factors.

The photovoltage enhancement on the SiNW appeared to have arisen from several factors. First, the positive shift in E_{OS} was partly attributed to the dramatically increased surface roughness of the SiNW,

$$\gamma = \frac{A_{\text{actual}}}{A} \tag{2}$$

where A_{actual} is the actual surface area of the SiNW/electrolyte interface and A is the projected area defined by the sealing. The actual value of γ for the SiNW/electrolyte interface can be estimated by measuring anodic oxide formation. Figure 3 shows

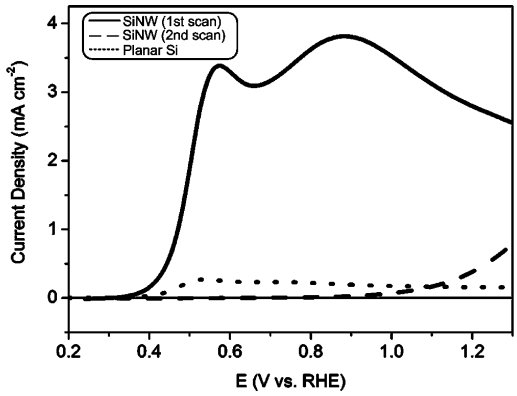

Figure 3. Linear sweep voltammograms of Si surface passivation in H_2SO_4 + 0.5 M K_2SO_4 (pH 1) at scan rate of 100 mV/s. The anodic current for SiNW (solid red) is much larger than that for planar Si, which is due to the dramatically increased surface area of the SiNW. Note that the anodic current is almost blocked in the second scan (dashed line), confirming a passiviting oxide has formed on Si surface during the first scan.

the $J-E$ measurements in the anodic passivation region, in which a thin surface oxide layer formed when E was scanned in the positive direction. When E was positive of 0.4 V, the SiNW electrode exhibited a much larger anodic current than the planar Si during the first scan. The $J-E$ results agreed with those reported previously[32] for Si anodic passivation in alkaline solution, although in an acidic environment the passivation peaks are broader and positioned toward more positive potentials. During the second scan, the anodic current was significantly inhibited due to the presence of a preformed anodic oxide layer that blocked further growth of the surface oxide. Because anodic passivation is a surface-limited process, the anodic charge passed during the anodic passivation should be proportional to the surface area. The anodic charge densities for the SiNW and the planar Si were 27 and 1.7 mC/cm^2, respectively. Assuming a γ value for the planar Si of 1, the γ value for the SiNW was estimated to be 16 from the ratio of the measured charge densities.

Regarding the photovoltage at the semiconductor/electrolyte interface, the value of γ can have both positive and negative effects. On the positive side, a large γ means a proportionally large electrode/electrolyte interface area adjacent to the redox molecules. The highly porous SiNW photocathode should then have a much lower local current density ($J_{\text{local}} = J/\gamma$) than the

dx.doi.org/10.1021/nl203564s | Nano Lett. 2012, 12, 298–302

planar Si when the apparent current levels in both electrodes are the same, which results in a lower overpotential. Deposition of the Pt electrocatalyst onto the extremely rough surface morphology of the SiNW surface to form Pt-impregnated SiNWs results in an average deposited Pt NP size that is much smaller than the average size of Pt NPs deposited on the planar Si. In accordance with a previous study,[31] the Pt NPs deposited onto SiNWs have an average diameter of 5−10 nm (see the Supporting Information for details), whereas the Pt NPs on the planar Si can be as large as 50 nm and can coalesce to some extent.[12] This observation indicates that for a given amount of Pt, the Pt surface area is expected to be much higher in the well-dispersed Pt/SiNW substrate than in the planar counterpart. As a useful analogy, this situation can be thought of as comparable to heterogeneous catalysis on a porous material, as occurs in fuel cell electrodes, where Pt NPs are dispersed on a fine carbon powder to maximize the surface area and specific activity of the precious metal catalyst.[33] On the negative side, a higher value for γ can dilute the concentration of the photogenerated minority carriers along the large semiconductor/electrolyte interface area, leading to a lower quasi-Fermi level and, therefore, a smaller photovoltage.[4]

In addition to the high surface roughness of the SiNWs, which contributes to the enhanced onset potential, the interfacial energetics of Si also may significantly affect the photovoltage. Figure 4 shows cyclic voltammograms of

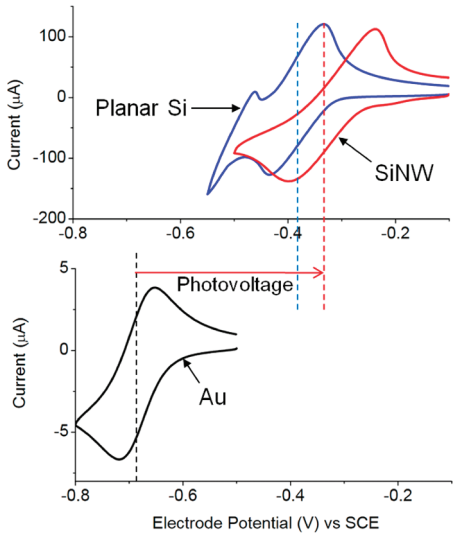

Figure 4. Cyclic voltammograms of methylviologen ($MV^{2+/+}$) in a quiescent solution of 2 mM $MVCl_2$ and 0.1 M KCl at scan rate of 50 mV/s. Illuminated SiNW and planar Si photocathodes exhibit significant photovoltage as measured to bare Au electrode. A photovoltage of +0.36 V is observed on Si NW, compared to +0.31 V on planar Si. The larger photovoltage on SiNW can be attributed to favorable (positive) shift of flat-band potential in SiNW compared to planar Si.

methylviologen ($MV^{2+/+}$) on SiNW as compared to the planar Si surface. To determine the magnitude of the photovoltage, a cyclic voltammogram of MV on bare Au electrode was also measured as a reference. Compared to the bare Au electrode, on which MV underwent a redox reaction at the expected formal potential ($E^{\circ\prime}$), the illuminated SiNW and planar Si photoelectrodes exhibited significant photovoltages. (The photovoltage was taken as the difference between the values of $E^{\circ\prime}$ for $MV^{2+/+}$ on the Si photoelectrodes and $E^{\circ\prime}$ on the Au bare electrode.) The photovoltage on the SiNW was 0.36 V, whereas that on the planar Si was slightly lower, 0.31 V. Note that electron transfer between the photoelectrode and $MV^{2+/+}$ was fast enough that the measured photovoltage was not significantly affected by the kinetic overpotential, but rather arose from the energetics of the Si/electrolyte interface. The maximum obtainable photovoltage can be estimated by[34]

$$\text{Photovoltage (max)} = |E_{FB} - E_{Redox}| \quad (3)$$

where E_{FB} is the flat-band potential, the electrode potential when there is no band bending in the semiconductor, and E_{Redox} is the redox potential of the $MV^{2+/+}$ couple. From eq 3, it can be deduced that the small but measurable difference between the photovoltages of the SiNW and planar Si substrates in Figure 4 was likely to have arisen from a more positive E_{FB} value in the SiNW, contributing to a higher photovoltage during H_2 generation. The reason for the E_{FB} shift is not clear at this time but is probably related to H^+ adsorption to the high-surface-area SiNWs. It is expected that a higher degree of adsorption of H^+ ions onto the highly porous SiNW surface would lead to a positive potential shift. Previous reports on porous Si have described a similar shift in E_{FB}, which was attributed to surface ion adsorption.[24]

Finally, aside from the reduced overpotential and favorable shift in E_{FB}, the light-trapping or antireflection effects of the high-surface-roughness SiNWs can contribute to enhanced photovoltages at a SiNW photocathode. Because of the large difference in the refractive indices of Si and water, the planar Si/water interface reflects as much as 25% of the incident visible light.[25] It would be very difficult or impossible to introduce an antireflection layer similar to that used in solid-state solar cells to the semiconductor/electrolyte interface because such a layer would easily block interfacial electron transfer. The dimensions of the periodic nanostructures in nanostructured semiconductors, such as the SiNW used in this work, are comparable to the wavelength of visible light and should significantly reduce photon reflection at the interface, as confirmed by visual observation of the black surface of the SiNW compared to the mirrorlike surface of the planar Si (see the inset in Figure 1a).

In conclusion, a novel photocathode based on SiNWs was successfully fabricated via the chemical etching of bulk Si materials. When the SiNW surface was modified with a Pt electrocatalyst, the Pt/SiNW photocathode exhibited a dramatically enhanced photovoltage compared to the planar Si, which was attributed to the extremely high surface roughness, positive shift in E_{FB}, and light-trapping by the low-reflectance SiNW. To our knowledge, the photovoltage of 0.42 V measured on the Pt/SiNW surface is the highest value ever reported for a Si/electrolyte interface during H_2 generation and should be of critical importance in realizing tandem photoelectrochemical cells for water splitting by relieving the photovoltage burden on the photoanode. Although current investigations are focused on the Si-based nanowire geometry, we expect that a variety of nanostructures, including nanopores and semiconductor materials other than Si, can be utilized to enhance the H_2 generation performance of semiconductor/electrolyte interfaces.

■ ASSOCIATED CONTENT

Ⓢ Supporting Information

Experimental details, SEM images of Pt/SiNW, and current−time response of H_2 evolution on Pt/SiNW for long-term

dx.doi.org/10.1021/nl203564s | Nano Lett. 2012, 12, 298−302

stability. This material is available free of charge via the Internet at http://pubs.acs.org.

AUTHOR INFORMATION

Corresponding Author

*E-mail: (I.O.) ioh0204@gmail.com; (S.H.) shwang@mju.ac.kr.

Author Contributions

[§]These authors contributed equally to this work.

ACKNOWLEDGMENTS

S.H. acknowledges the support from Basic Science Research Program through the National Research Foundation of Korea (NRF) funded by the Ministry of Education, Science, and Technology (2011-0003612).

REFERENCES

(1) Turner, J. A. *Science* **2004**, *305*, 972−974.
(2) Bard, A. J.; Fox, M. A. *Acc. Chem. Res.* **1995**, *28*, 141−145.
(3) Heller, A. *Acc. Chem. Res.* **1981**, *14*, 154−162.
(4) Walter, M. G.; Warren, E. L.; McKone, J. R.; Boettcher, S. W.; Mi, Q.; Santori, E. A.; Lewis, N. S. *Chem. Rev.* **2010**, *110*, 6446−6473.
(5) *Handbook of photovoltaic science and engineering*; Luque, A., Hegedus, S., Eds.; John Wiley & Sons: West Sussex, 2003.
(6) Bookbinder, D. C.; Lewis, N. S.; Bradley, M. G.; Bocarsly, A. B.; Wrighton, M. S. *J. Am. Chem. Soc.* **1979**, *101*, 7721−7723.
(7) Bocarsly, A. B.; Bookbinder, D. C.; Dominey, R. N.; Lewis, N. S.; Wrighton, M. S. *J. Am. Chem. Soc.* **1980**, *102*, 3683−3688.
(8) Bookbinder, D. C.; Bruce, J. A.; Dominey, R. N.; Lewis, N. S.; Wrighton, M. S. *Proc. Natl. Acad. Sci.* **1980**, *77*, 6280−6284.
(9) Nakato, Y.; Egi, Y.; Hiramoto, M.; Tsubomura, H. *J. Phys. Chem.* **1984**, *88*, 4218−4222.
(10) Boettcher, S. W.; Spurgeon, J. M.; Putnam, M. C.; Warren, E. L.; Turner-Evans, D. B.; Kelzenberg, M. D.; Maiolo, J. R.; Atwater, H. A.; Lewis, N. S. *Science* **2010**, *327*, 185−187.
(11) Peng, K.-Q.; Lee, S.-T. *Adv. Mater.* **2011**, *23*, 198−215.
(12) Boettcher, S. W.; Warren, E. L.; Putnam, M. C.; Santori, E. A.; Turner-Evans, D.; Kelzenberg, M. D.; Walter, M. G.; McKone, J. R.; Brunschwig, B. S.; Atwater, H. A.; Lewis, N. S. *J. Am. Chem. Soc.* **2011**, *133*, 1216−1219.
(13) Czaban, J. A.; Thompson, D. A.; LaPierre, R. R. *Nano Lett.* **2009**, *9*, 148.
(14) Dong, Y.; Tian, B.; Kempa, T.; Lieber, C. M. *Nano Lett.* **2009**, *9*, 2183.
(15) Fan, Z.; Razavi, H.; Do, J.; Moriwaki, A.; Ergen, O.; Chueh, Y.; Leu, P.; Hol, J.; Takahashi, T.; Reichertz, L.; Neale, S.; Yu, K.; Wu, M.; Ager, J.; Javey, A. *Nat. Mater.* **2009**, *8*, 648.
(16) Garnet, E.; Yang, P. D. *Nano Lett.* **2010**, *10*, 1082.
(17) Garnett, E. C.; Yang, P. D. *J. Am. Chem. Soc.* **2008**, *130*, 9224.
(18) Han, S. E.; Chen, G. *Nano Lett.* **2010**, *10*, 1012.
(19) Muskens, O. L.; Rivas, J. G.; Algra, R. E.; Bakkers, E. P. A. M.; Lagendijk, A. *Nano Lett.* **2008**, *8*, 2638.
(20) Peng, K. Q.; Wang, X.; Wu, X. L.; Lee, S. T. *Nano Lett.* **2009**, *9*, 3704.
(21) Sivakov, V.; Andra, G.; Gawlik, A.; Berger, A.; Plentz, J.; Falk, F.; Christiansen, S. H. *Nano Lett.* **2009**, *9*, 1549.
(22) Yuhas, B.; Yang, P. D. *J. Am. Chem. Soc.* **2009**, *131*, 3756.
(23) Yuan, G.; Aruda, K.; Zhou, S.; Levine, A.; Xie, J.; Wang, D. *Angew. Chem., Int. Ed.* **2011**, *50*, 2334−2338.
(24) Koshida, N.; Echizenya, K. *J. Electrochem. Soc.* **1991**, *138*, 837.
(25) Oh, J.; Deutsch, T. G.; Yuan, H.-C.; Branz, H. M. *Energy Environ. Sci.* **2011**, *4*, 1690.
(26) Yan, R.; Gargas, D.; Yang, P. *Nat. Photonics* **2009**, *3*, 569−576.
(27) Maiolo, J. R. III; Kayes, B. M.; Filler, M. A.; Putnam, M. C.; Kelzenberg, M. D.; Atwater, H. A.; Lewis, N. S. *J. Am. Chem. Soc.* **2007**, *129*, 12346−12347.
(28) Peng, K.; Yan, Y.; Gao, S.; Zhu, J. *Adv. Funct. Mater.* **2003**, *13*, 127−132.
(29) Peng, K.-Q.; Yan, Y.-J.; Gao, S.-P.; Zhu, J. *Adv. Mater.* **2002**, *14*, 1164−1167.
(30) Hochbaum, A. I.; Chen, R.; Delgado, R. D.; Liang, W.; Garnett, E. C.; Najarian, M.; Majumdar, A.; Yang, P. *Nature* **2008**, *451*, 163−167.
(31) Peng, K.-Q.; Wang, X.; Wu, X.-L.; Lee, S.-T. *Nano Lett.* **2009**, *9*, 3704−3709.
(32) Chen, L. C.; Chen, M.; Wan, C. C. *J. Electrochem. Soc.* **1995**, *142*, 170.
(33) Kinoshita, K. *Carbon: Electrochemical and Physicochemical Properties*; John Wiley & Sons, New York, 1993.
(34) Zhang, X. G. *Electrochemistry of Silicon and Its Oxide*; Kluwer: New York, 2001.